

# Dc and un SQUIDs for Readout of ac-biased Transition-Edge Sensors

Mikko Kiviranta, Jari S. Penttilä, Leif Grönberg, Heikki Seppä and Ilkka Suni

**Abstract**— We have developed a set of SQUIDs optimized for readout of ac-biased transition edge sensors. Junction shunts are made of Pd and attached to cooling fins to facilitate low-noise operation at sub-kelvin temperatures. SQUIDs have a low loop inductance in order to reach a large natural dynamic range even without negative feedback. The SQUIDs are intended to be used for frequency-domain multiplexing of X-ray calorimeter arrays. Both traditional dc SQUIDs and novel un SQUIDs are manufactured. The fabrication process and SQUID design criteria are reviewed.

## I. INTRODUCTION

Imaging arrays of Transition Edge Sensors (TESes) are intended to be used as detectors for astronomical cameras in far infrared and X-ray regions of the electromagnetic spectrum. Array readout requires in practice either time-domain multiplexing (TDM) [1] or frequency-domain multiplexing (FDM) [2], whose large bandwidths set strict requirements to the performance of the readout SQUID. We have designed and fabricated a set of new SQUIDs, taking into account the special requirements present in FDM multiplexers for TES arrays. There are un- and dc-SQUID variants in the mask set. The design of the un SQUID variant is based on experimental results from our older un SQUID version.

### A. Dynamic range

X-ray detectors are typically single photon counters, whose (dc-biased) output current has a dynamic range  $D = 2.36 \times E_{\max}/(\Delta E_{\text{FWHM}}\sqrt{\tau_i})$  determined by maximum photon energy  $E_{\max}$ , required energy resolution  $\Delta E_{\text{FWHM}}$  and integration time  $\sqrt{\tau_i}$ . Typically the need for dynamic range on unit bandwidth is  $D = 10^6 \dots 10^7$ . Furthermore, linearity requirement dictates that flux applied to the SQUID should not exceed  $\sim 5\%$  of the full flux range of half flux quantum  $\Phi_0/2$ . In single-pixel readouts sufficient dynamic range can be arranged by negative feedback from the readout amplifier, but this becomes difficult in multiplexing schemes, because of the greater need for bandwidth.

Natural dynamic range of the dc SQUID is the ratio of  $\Phi_0/2$  to the flux noise

$$\Phi_n = \sqrt{2\varepsilon L_{\text{SQ}}} = \sqrt{24k_B T L_{\text{SQ}} \sqrt{L_{\text{SQ}} C_j}}, \quad (1)$$

Presented in the Applied Superconductivity Conference (ASC'02), Houston, Texas, 4-9 August, 2002. This work was supported in part from the Antares program by TEKES the National Technology Agency of Finland. Authors are with VTT Information Technology, Tietotie 3, FIN-02150 Espoo, Finland. M. Kiviranta can be contacted by email: Mikko.Kiviranta@vtt.fi.

but this is multiplied by the loop gain of the complete readout circuit  $A_V$  if negative feedback is used. In (1)  $\varepsilon$  is the energy resolution, bounded from below by  $\sim \hbar$ ,  $L_{\text{SQ}}$  and  $C_j$  are the loop inductance and junction capacitance of the SQUID,  $k_B$  is Boltzmann's constant and  $T$  is the shunt resistor temperature.

In order to make the feedback loop stable, the loop gain as a function of frequency must fall below unity before cable delay starts to produce too much phase shift. Because loop gain cannot increase faster than 40 dB/dec when frequency is lowered below the unity-gain frequency<sup>1</sup>, it is difficult to obtain large loop gains at high frequencies. Thus it is useful to have a SQUID with a large natural dynamic range, i.e. a SQUID with small flux noise. As seen from (1), the natural dynamic range can be improved by decreasing  $L_{\text{SQ}}$  even when the energy resolution has reached the quantum limit.

Usually, the noise level and subsequently the dynamic range is not dominated by the internal flux noise of the SQUID, but rather, by noise due to the readout amplifier and Johnson noise in the cabling. It is then advantageous to have a SQUID with large gain. A second SQUID stage to increase gain is conceivable, but then the dynamic range would be limited by the (possibly amplifier dominated) flux noise of the second SQUID alone<sup>2</sup>.

### B. Energy resolution

The maximum load inductance tolerated by the TES is limited by the thermal stability condition [4]. In a single-pixel readout all the inductance can be coupled to the SQUID, but in a  $N$ -pixel current-summing FDM multiplexer [5] only fraction  $1/N$  of the tolerated inductance can couple to the SQUID, because the common inductance sets the total bandwidth available to all  $N$  channels. In order to reach noise-equivalent input current  $i_{n,\text{SQ}}$  below the TES noise  $i_{n,\text{TES}}$ , simultaneously with low input inductance  $L_{in}$ , one must improve the energy resolution  $\varepsilon = L_{in} i_{n,\text{SQ}}^2$  of the SQUID  $N$ -fold over the the single-pixel case. This effect results in a noise penalty equivalent to the penalty present in the TDM approach [1].

### C. Heat dissipation

In space-based missions, such as XEUS [3], available cooling power is limited. If SQUIDs are located at base temperature

<sup>1</sup>In practice, it is difficult to exceed 30 dB/dec obtainable with the integrator-and-half. Often a simple integrator with 20 dB/dec slope is used.

<sup>2</sup>SQUID series arrays are sometimes used as second stages because of their large natural dynamic range. A  $k$ -SQUID series array, each SQUID with loop inductance  $L_{\text{SQ}}$ , junction capacitance  $C_j$ , and coupled to an  $m$ -turn input coil, can be shown to have the same small-signal parameters as a single SQUID with  $L_{\text{SQ}}/k$  loop inductance,  $kC_j$  junction capacitance,  $km$ -turn input coil and  $1:k$  transformer at its output.

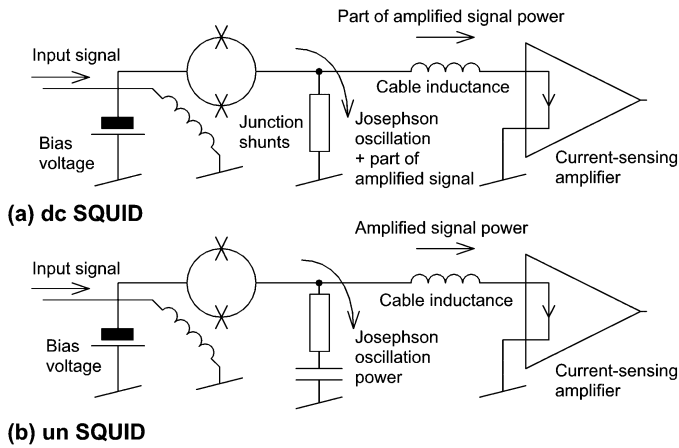


Fig. 1. Schematic power flow in dc SQUID and un SQUID.

of the refrigerator, either in order to reduce noise or to simplify the TES-to-SQUID wiring, the SQUID heat production becomes an issue. Unfortunately, according to a simple estimate the dynamic range and power dissipation of a dc SQUID are related approximately by  $P = 14k_B T \times D^2$ , or 200 pW for a SQUID with  $D = 10^7$  at 1 kelvin.

## II. UNSHUNTED SQUID

The traditional dc SQUID can be approximated as a superconducting ring broken by two unshunted junctions (Fig. 1a), coupled in parallel with a resistor. The resistor serves two functions: it (i) provides dissipation at Josephson frequency, and (ii) provides sufficiently low source impedance for stable biasing<sup>3</sup> of the junction ring, whose natural dynamic impedance is negative. One disadvantage of the setup is that more than half of the signal power generated by the junction ring is wasted away in the resistor before it ever reaches the readout amplifier. The result is excess heat generation and loss of available power gain.

In a more attractive setup (Fig. 1b) only the Josephson oscillation is dissipated in the shunt resistor, but signal power at lower frequencies is all fed to the readout amplifier. The amplifier effectively reads the current which would flow through the shunt resistor if one were present. The voltage-to-current characteristics seen by the amplifier can be approximated by subtracting a resistive line (due to the missing current through shunt resistors) from characteristics of a traditional dc SQUID. The resulting characteristics have negative resistance, so that voltage bias must be used for stable operation. The device is called unshunted SQUID (un SQUID) [6].

General usability of the concept has been checked with our older un SQUID design [7]. When read out directly with an AD797 operational amplifier (Fig. 2a), white noise level of  $6 \mu\Phi_0/\sqrt{\text{Hz}}$  was measured, which corresponds to the current induced in the  $R_d \approx -3.5 \Omega$  dynamic resistance by the  $1 \text{ nV}/\sqrt{\text{Hz}}$  voltage noise of the op amp. When the device was coupled in parallel with a  $4.3 \Omega$  resistor (Fig. 2b), white noise level dropped to  $2 \mu\Phi_0/\sqrt{\text{Hz}}$ , which is explained by the increase of  $|R_d|$  and subsequent decrease in the current fluctuation induced

<sup>3</sup>The low-impedance requirement is in close analogy to stable biasing of a TES, whose characteristics, too, have a region of negative dynamic resistance.

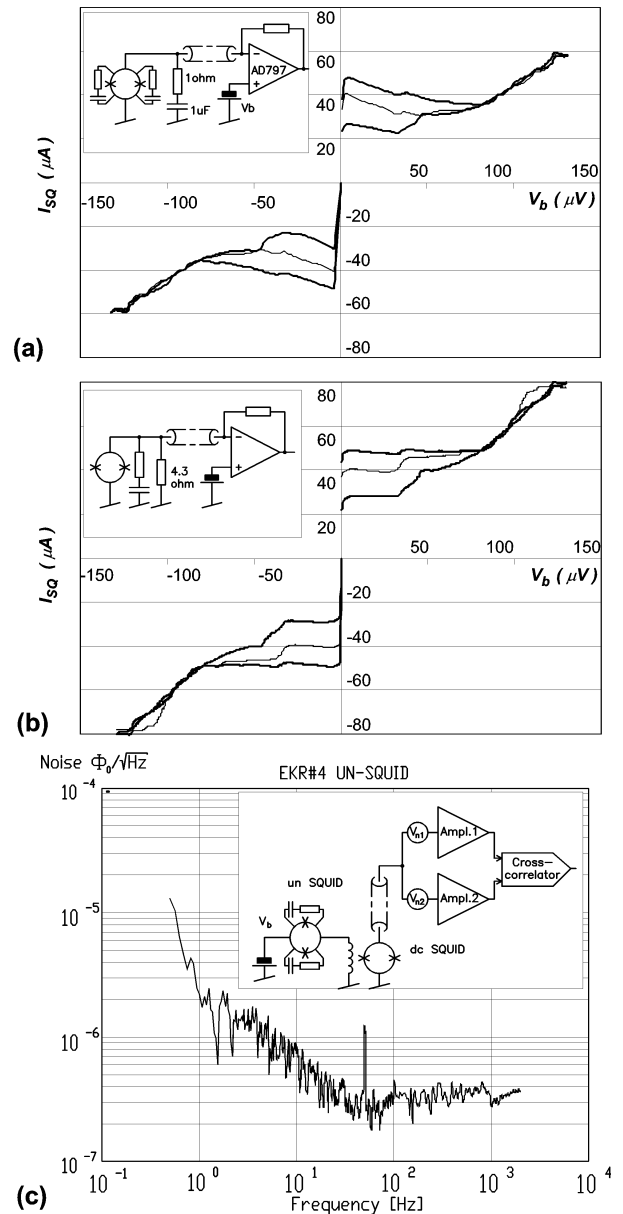


Fig. 2. (a) Current characteristics of a un SQUID as a function of bias voltage at applied flux values  $0$ ,  $\Phi_0/4$  and  $\Phi_0/2$ . An ordinary operational amplifier is used for readout. There are  $1.6 \Omega$  on-chip junction shunts in series with  $100 \text{ pF}$  capacitors, and a  $1 \Omega / 1 \mu\text{F}$  damping circuit made of SMD components at the  $4.2\text{K}$  stage. (b) Characteristics of the same un SQUID with an additional  $4.3 \Omega$  resistor. (c) Flux noise of a similar device, equipped with an on-chip readout SQUID, read out using a cross-correlation technique.

by the amplifier noise. White noise level of a similar device was  $0.35 \mu\Phi_0/\sqrt{\text{Hz}}$  (Fig. 2c) when measured by a second SQUID stage and using a cross-correlation technique [7]. Noise measurements were performed at  $4.2 \text{ K}$ .

## III. SQUID FABRICATION

### A. Process

The new set of SQUIDs has been designed and fabricated using a process with ion-mill patterned Pd resistors, a Nb-AlOx-Nb trilayer with critical current density  $J_c = 10^7 \text{ A/m}^2$ , and further two Nb metallization layers. Pd is grown on AlN sacrificial layer which is chemically removed after the ion milling

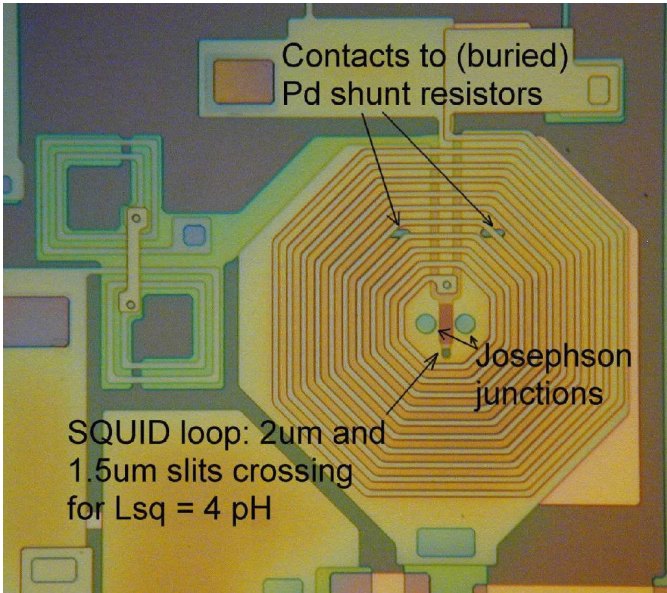


Fig. 3. Microphotograph of a washer-type dc SQUID with a low loop inductance.

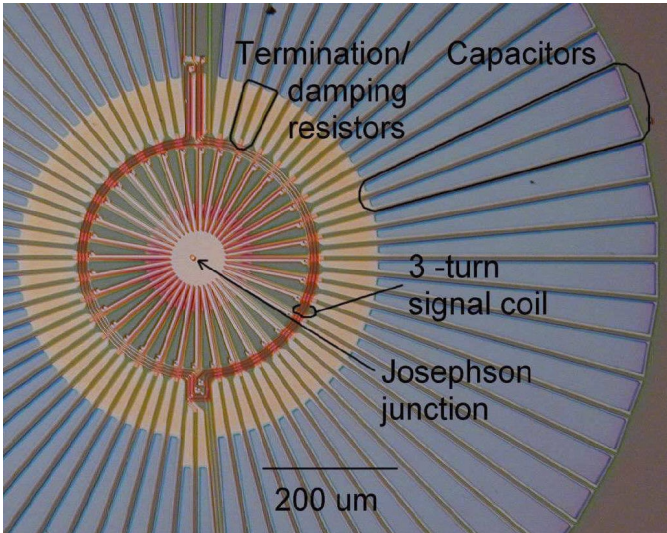


Fig. 4. Microphotograph of a fractional-turn un SQUID. The junction ring is divided into 36 parallel-coupled loops to obtain an estimated  $\sim 1$  pH inductance. Only one of the  $\text{\O}11 \mu\text{m}$  junctions can be seen in the middle: the second junction gets hidden in the CMP planarization step.

step, for the purpose of obtaining a smooth surface for subsequent layers. Junctions are defined by plasma etching, followed by a light anodization step. The  $\text{Nb}_2\text{O}_5$  capacitor dielectric is formed in the anodization step, but Al-AIOx is removed before anodization so that low-permittivity aluminum oxide is not present in the dielectric stack. We estimate that capacitance densities in the order of  $C_D = 0.01 \text{ F/m}^2$  are achievable. Superconducting layers are insulated from each other by low-temperature PECVD silicon dioxide. Contact windows are etched in  $\text{CHF}_3/\text{O}_2$  plasma. Chemical-mechanical polishing (CMP) planarization is applied after insulation layer deposition, in order to improve step coverage and obtain superconducting traces which can tolerate large current densities. TES signal

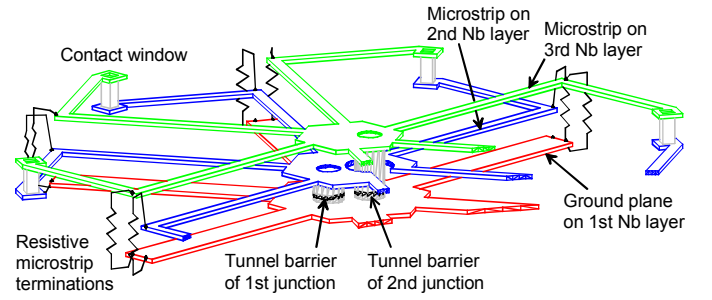


Fig. 5. Schematic arrangement of the multiloop un SQUID consisting of 6 subloops. The radial transmission lines feeding the circumference of the fractional-turn loop are terminated by R- or RC-shunts, which also act as damping for Josephson frequency. There are no traditional shunt resistors close to the junctions.

currents may be large, and a large critical current for Josephson junctions is implied by the low loop inductance.

### B. Design

Simple calculations, derived from well-known analytic formulas for optimal-noise ( $\beta_C = 2\pi R_s^2 I_c C_j / \Phi_0 = 1$  and  $\beta_L = 2L_{\text{SQ}} I_c / \Phi_0 = 1$ ) autonomous dc SQUIDS, yield order-of-magnitude estimates for design parameters and their scaling as function of external constraints. More complicated formulas as well as numerical simulation have been used in the detailed device design. Because the relevant gain figure in the case of power-matched readout amplifier, i.e. ratio of available power  $P_a$  at SQUID output to applied flux  $\Phi_a$ , is approximately  $\sqrt{\Delta P_a} = \Delta \Phi_a \times \frac{1}{2} L_{\text{SQ}}^{-3/4} C_j^{-1/4}$ , amplifier noise is taken into account by simply replacing  $T$  in (1) and in equations derived from it by  $T_a/3$  where  $T_a$  is noise temperature of the amplifier.

Dynamic range requirement  $D$  (which should include the reserve for linearization) and available loop gain  $A_V$  of the feedback electronics at highest operating frequency determine loop inductance by

$$L_{\text{SQ}} = \frac{\Phi_0^2 A_V^2 \omega_{LC}}{96 k_B T D^2}. \quad (2)$$

Note that the LC-resonance frequency  $\omega_{LC} = (L_{\text{SQ}} C_j)^{-1/2}$  gets fixed by the trilayer properties: the critical current density  $J_c$  and sheet capacitance  $C_T$  of the tunneling barrier, so that  $\omega_{LC} = (C_T \beta_L \Phi_0 / 2 J_c)^{-1/2}$ . Two distinct approaches has been taken in order to reach low loop inductances. In first approach, ordinary washer-style SQUIDS are fabricated. The inductance is determined by crossing slits in two superconducting planes, and estimated to be  $\sim 4$  pH (Fig. 3). In second approach the loop is divided into several parallel sub-loops [8] for an estimated total loop inductance of  $\sim 1$  pH (Figs. 4 and 5).

Lower limit to the number of turns in the input coil  $n$  is then defined by requiring that the system is dominated by TES current noise  $i_{n,\text{TES}}$  rather than SQUID noise

$$n = 48 \frac{\zeta k_B T D}{i_{n,\text{TES}} \omega_{LC} A_V \Phi_0}. \quad (3)$$

The parameter  $\zeta = 1 \dots 3$  sets the a safety margin between SQUID noise and TES noise.

An upper limit to the number of turns is set by two factors. (i) Back-action noise from the SQUID should not become a dominant factor. A rough estimate for the back-action noise voltage at frequency  $\omega$  is  $u_n \simeq \omega n \sqrt{2k_B T L_{SQ} \xi}$ , which also sets an ultimate upper limit to the operating frequency for the TES readout. (ii) The SQUID input inductance (screened by negative feedback) seen by the TESes  $L_{in} \simeq n^2 L_{SQ} / A_V$  must be sufficiently low, because common inductance limits the available total bandwidth and thus the number of TESes that can be multiplexed with one SQUID.

Because number of turns in the input coil tends to be rather low,  $n \simeq 2 \dots 10$ , owing to the low source impedance presented by the TES, resonances associated with the input coil are at high frequencies. Because  $RI_c$ -product which sets the Josephson frequency at typical bias points tends to be high in low- $\Phi_n$  devices, the resonance frequencies are not well separated from Josephson frequency. Damping of the resonances is then necessary.

In addition to flux side resonances, the bias side resonances may cause excess noise, especially in un SQUIDs where less damping is naturally present. Some versions of our devices contain an on-chip transformer at the SQUID output, designed to drive a  $50 \Omega$  line. The parasitic resonances of the transformer are modelled with a general-purpose circuit simulator Aplaac, and suitable damping is arranged.

Resistors in the devices are made of palladium for sub-kelvin operation. Furthermore, junction shunts are designed to have large volume so that electron systems of the resistors cool sufficiently even at temperatures where electron system starts to decouple from phonon system [9]. Owing to the low  $L_{SQ}$  it is sufficient to reach  $T_{electr} \simeq 0.2 \dots 0.4$  K, below which the SQUIDs would theoretically be quantum rather than thermally limited. Note that reduced dissipation in un SQUIDs further alleviates the need for resistor volume.

### C. Measurements

Voltage-to-current and flux-to-current characteristics of a multiloop un SQUID are shown in Fig. 6. The simplest way to obtain stable characteristics for a un SQUID is to use an external resistor close to the SQUID chip as a junction shunt and thus effectively transform the un SQUID into a dc SQUID: this is the method used to obtain the characteristics in Fig. 6.

Noise measurements have not been performed.

## IV. CONCLUSION

We have fabricated a set of SQUID devices, designed for reading out an frequency-multiplexed array of superconducting transition-edge sensors in X-ray calorimeter configuration. The devices are designed for high dynamic range operation at high frequencies where it is difficult to obtain negative feedback because of cable delay present between the room-temperature electronics and the cryogenic stage. The SQUIDs are capable to reside at a base temperature of a millikelvin refrigerator. In addition to traditional dc SQUIDs, novel devices called un SQUIDs have been fabricated. Un SQUIDs are even better suited for TES readout owing to their large gain and low heat production.

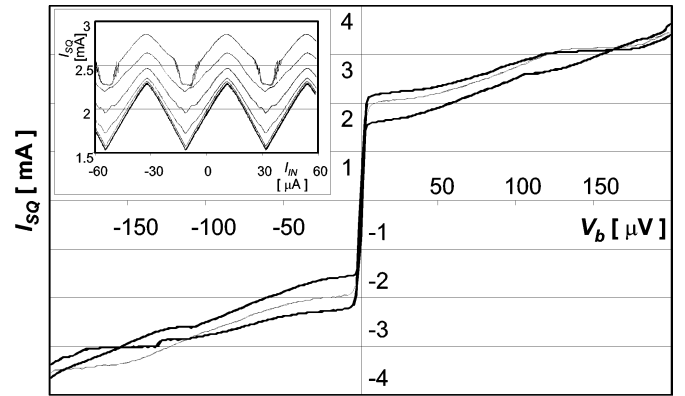


Fig. 6. Current of a multiloop un SQUID depicted in Fig. 4 as a function of bias voltage, when coupled in parallel with a  $0.1 \Omega$  off-chip SMD resistor. In the inset the SQUID current is shown as a function of the current through the 3-turn signal coil, when bias voltage is  $V_b = 10, 20, 40, 60, 80$  and  $100 \mu V$ .

## V. ACKNOWLEDGEMENTS

M. Kiviranta thanks Dr. Jan van der Kuur for valuable discussions and Mr. Vesa Virkki for the cross correlation -based noise measurement.

## REFERENCES

- [1] K. Irwin, "SQUID multiplexers for transition-edge sensors," *Physica C*, vol. 368, pp. 203-210, 2002.
- [2] M. Kiviranta, H. Seppä, J. van der Kuur and P. de Korte, "SQUID-based readout schemes for microcalorimeter arrays," Proceedings of the 9th international workshop on low temperature detectors (LTD-9), *AIP Conference Proceedings*, vol. 605, pp. 295-300, 2002. J. Yoon et al. "Single SQUID multiplexer for arrays of voltage-biased superconducting bolometers," same proceedings, pp. 305-308. T. Miyazaki et al. "AC calorimeter bridge: a new multi-pixel readout method for TES calorimeter arrays," same proceedings, pp. 313-316.
- [3] <http://sci.esa.int/home/xeus/index.cfm>.
- [4] K. Irwin, G. Hilton, D. Wollman and J. Martinis, "Thermal-response time of superconducting transition-edge microcalorimeters," *J. Appl. Phys.*, vol. 83, p. 3978, 1998.
- [5] M. Kiviranta, J. van der Kuur, H. Seppä and P. de Korte, "SQUID multiplexers for transition-edge sensors," *Proceedings of the far-IR, sub-mm & mm detector technology workshop*, Monterey CA, 1-3 April 2002, in press.
- [6] H. Seppä, M. Kiviranta and L. Grönberg, "Dc SQUID based on unshunted junctions: experimental results," *IEEE Tran. Appl. Supercond.*, vol. 5, no. 2, pp. 3248-3251, June 1995.
- [7] H. Seppä et al. "Experiments with a un SQUID based integrated magnetometer," *Extended abstracts of the 6th International Superconductive Electronics Conference (ISEC'97), 25-28 June 1997, Berlin, Germany*, pp. 26-28.
- [8] J. E. Zimmerman, *J. Appl. Phys.*, vol. 42, p. 4483, 1971; D. Drung, *Appl. Phys. Lett.*, vol. 67, p.1474, September 1995. P. Carelli, M. Castellano, G. Torrioli, R. Leoni, *Appl. Phys. Lett.*, vol.72, pp. 115-117, January 1998.
- [9] F. C. Wellstood, *Ph.D. thesis*, University of Berkeley, October 1988.